Drug Design, Development and Therapy

Dovepress
Taylor & Francis Group

Open Access Full Text Article

ORIGINAL RESEARCH

Hirsutella sinensis Fungus Enhances CD8$^+$ T Cell Anti-Tumor Activity in NSCLC via Modulating the IL-10/STAT3/STAT1 Axis

Lei Zhang, Yanhui Xu, Jing Luo, Hongyu Lin, Lilong Xia*, Xinhai Zhu*

Department of Thoracic Surgery, Zhejiang Hospital, Hangzhou, People's Republic of China

*These authors contributed equally to this work

Correspondence: Lilong Xia; Xinhai Zhu, Department of Thoracic Surgery, Zhejiang Hospital, No. 1229 Gudun Road, Hangzhou, Zhejiang, 310030, People's Republic of China, Email xialilong181818@163.com; zxh.cool@163.com

Purpose: The tumor microenvironment (TME) has been shown to have a significant impact on lung cancer. Previously, *Hirsutella sinensis fungus* (HSF) may greatly boost T cell infiltration in the TME. In this study, we aimed to investigate HSF-mediated immunomodulation via IL-10 signaling in TME of non-small cell lung cancer (NSCLC).

Methods: An lung cancer mouse model was generated by subcutaneous injection of LLC cells with or without IL-10 knockdown in C57BL/6 mice or nude mice. HSF was orally administered once to the model mice daily for 15 days. Tumor growth was measured using in vivo imaging technology and vernier calipers. Hematoxylin and eosin (H&E) and Enzyme-linked immunosorbent assay (ELISA) were employed to estimate the cytotoxicity and immunological factors of the HSF treatment. Immune profiles, proliferation, apoptosis, the function of CD8$^+$ T cells, and the primary source of IL-10 in tumor tissue were detected by flow cytometry. RT-qPCR and Western blotting were performed to detect IL-10/STAT3/STAT1-related proteins in tumor tissues and CD8$^+$ T cells.

Results: HSF could inhibit tumor growth in LLC tumor model mice. Significantly, HSF reduced F4/80$^+$ CD11b$^+$ macrophages and regulatory T cells, as well as increased the percentage of Naïve T cells (CD44^{Low}CD62L^{High}) and central memory T cells (T(CM), CD44^{High}CD62L^{High}) populations in tumor tissues. Importantly, HSF inhibited apoptosis, and promoted cell proliferation and secretion of interferon (IFN)-γ and granzyme B in CD8$^+$ T cells, which were attenuated by IL-10. Western blot analysis of tumor tissues and CD8$^+$ T cells demonstrated that IL-10R, phosphorylation of STAT3 and STAT1 were significantly decreased upon HSF treatment. Flow cytometry identified B cells as the primary IL-10 source in tumor tissues.

Conclusion: HSF displayed antitumor immune activity by increasing the infiltration of CD8$^+$ T cells in vivo, which might be made feasible by down-regulation of the IL-10/STAT3/STAT1 signaling pathway.

Keywords: lung cancer, *Hirsutella sinensis* fungus, immunotherapy, IL-10

Introduction

In recent years, tumor immunotherapy has received significant attention for its efficacy in advanced tumors where conventional therapies have failed.[1,2] In particular, chimeric antigen receptor (CAR) modified T-cell (CAR-T) technology and immune checkpoint inhibitor therapies such as CTLA-4 and PD-1/PD-L1, which reverse the immunosuppressive function of tumors, have achieved exciting results in the treatment of solid tumors such as haematological tumors and melanoma respectively.[3–5] However, there are still many unanswered scientific questions in the field of tumor immunology. Predictably, future research will be more focused on how to improve the efficacy, increase the number of adaptive tumor types and control their immune-related adverse effects.

The success of tumor immunosurveillance and tumor immunotherapy is largely dependent on tumor-infiltration-activated CD8$^+$ T cells.[6] It has been shown that CD8$^+$ cytotoxic T cells could recognize point mutations in oncogenes and thus kill tumor cells, and therefore immunotherapy such as tumor vaccines or adaptive T-cell infusion aims to increase

Received: 17 April 2025
Accepted: 26 October 2025
Published: 6 November 2025

Graphical Abstract

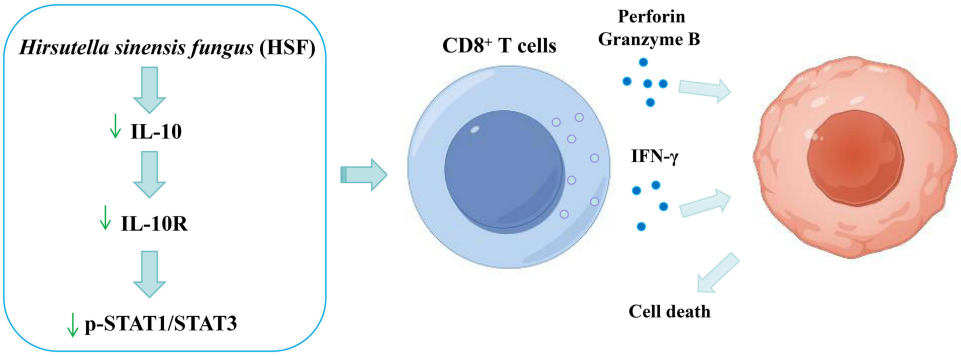

tumor-infiltrating T cells.[6,7] However, clinical studies have found that despite significant increases in endogenous or vaccine-induced tumor effector T circulating in the patient's system, there is no improvement in clinical outcomes. The reasons for this are twofold: 1) systemic circulating effector T cells do not infiltrate the tumor area and thus fail to kill tumor cells; 2) the immunosuppressive tumor microenvironment (TME). On the one hand, the tumor cells off-target effector $CD8^+$ T cells through low expression of major histocompatibility complex (MHC) molecules and tumor-associated antigens (TAAs); on the other hand, they secrete chemokines to recruit immunosuppressive cell aggregates, such as regulatory T cells Treg and myeloid-derived suppressor cells (MDSC), which inhibit the infiltration of effector T cells.[8,9] In summary, the immunosuppressive microenvironment not only suppresses the activity of effector T cells but also blocks the infiltration of effector T cells and plays an important role in immune tolerance. Therefore, modifying the immunosuppressive microenvironment and enhancing tumor-infiltrating effector T cells are currently the most critical core aspect to improve the efficacy of immunotherapy.

The GLOBOCAN 2022 cancer report[10] shows that lung cancer will lead the world in 2022 with a mortality rate of 18.7% and an incidence rate of 12.4%. According to the Cancer statistics in China and the United States, 2022, the number of lung cancer cases and deaths in China account for 37.0% and 45.2% of the world's lung cancer cases, respectively.[10,11] Lung cancer can be divided into non-small cell lung cancer (NSCLC) and small cell lung cancer according to histopathology, with the incidence of NSCLC accounting for 80% to 85% of lung cancer.[12] Modern medical treatment for NSCLC patients includes molecularly targeted drugs and immune checkpoint inhibitors, which have achieved certain efficacy, but there are still problems such as negative driver gene sensitivity, resistance to targeted drug therapy,[13] and adverse reactions to immune checkpoint inhibitors.[14] In contrast, Traditional Chinese medicine (TCM) has its characteristics in inhibiting tumor growth and metastasis, reducing tumor load, and regulating patients' immune function,[15] which has an important role in improving patients' survival quality and prognosis. Cordyceps sinensis is a valuable traditional Chinese herbal medicine in China, which was first published in the 《new compilation of materia medica》, and has the function of tonifying the lungs and benefiting the kidneys. Early on, Chinese experts observed the effect of Cordyceps on lung cancer chemotherapy in the elderly and found that Cordyceps could relieve the symptoms of weakness after chemotherapy and reduce the complications caused by immune deficiency after chemotherapy.[16,17] *Hirsutella sinensis* Liu, Guo, Yu et Zeng (1989) is an asexual strain of *Cordyceps sinensis* isolated from Qinghai Cordyceps by researcher Shen Nanying in the early 1980s, and its industrialized artificial Cordyceps powder has been approved by SFDA in China, such as Bailing capsule, which is used as a clinical substitute for Cordyceps sinensis in treating various diseases.[18] Through clinical observation of *Hirsutella sinensis* Fungus (HSF) with chemotherapy for intermediate and advanced malignant tumors (eg breast cancer, lung cancer, gastric cancer, etc)., researchers have shown that HSF could reduce the bone marrow suppression caused by radiotherapy, increase the peripheral blood leucocytes of patients, improve the tolerance of chemotherapy, and enhance the immune function of tumor patients.[19,20] Modern pharmacological studies have demonstrated that HSF could inhibit a variety of

pharmacological effects in mice mainly through enhancing immune function and improving the levels of various cytokines, such as IFN-γ and IL-2.[21,22] And, these are key factors in promoting T cell proliferation and production of the T cell effect, suggesting that the anti-tumor effects of HSF are related to T cells.

Interleukin-10 (IL-10), a classical immunosuppressive cytokine, is produced by cells of the innate and adaptive immune system, including T cells, B cells, macrophages, and neutrophils, and is not only associated with inflammation and infection in the body but is also involved in the regulation of tumor immunity in the body.[23,24] Current studies have shown that IL-10 has complex impacts on tumor growth, displaying both anti-tumor and pro-tumor effects, so its tumor regulation is still controversial,[25] and this difference may be related to differences in cancer type and tumor microenvironment. More recently, Shiri et al found that IL-10 suppresses antitumor immune responses and facilitates liver metastasis by inducing PD-L1.[26] Furthermore, IL-10-producing B (B10) cells promote carcinogenesis in gastric cancer.[27] However, a study of Wang et al demonstrated that IL-10 overexpression decreased tumor growth in breast cancer by modulating the IL-10-CXCL5-MDSCs axis.[28] In general, IL-10 has been reported to play an important immunomodulatory role in the development of breast, colorectal and gastric cancers,[29,30] but its regulatory role in lung cancer is still poorly reported. Combined with the group's previous work, we hypothesized that HSF may promote the expansion of effector T cells in the tumor microenvironment through IL-10, thus exerting anti-tumor effects.[21] In this study, we used this hypothesis to explore the regulatory mechanism of HSF on IL-10-mediated tumor effector T cells, to clarify the regulatory mechanism of HSF on CD8 T cells, to elucidate the mechanism of HSF's anti-tumor immune action, and to provide experimental evidence and theoretical basis for the secondary development of HSF.

Materials and Methods

Cell Culture

Lewis lung cancer (LLC) and LLC luciferase (LLC-Luc) cells were purchased from iCell Bioscience Inc (Shanghai, China). LLC and LLC-Luc cells were cultured in Dulbecco's modified Eagle's medium (DMEM, Gibco, USA) with 10% fetal bovine serum (FBS; Hangzhou Sijiqing Biological Engineering Materials Co., Ltd. Zhejiang, China) and 5% penicillin-streptomycin at 37°C in a 5% CO_2 humidified atmosphere.

Animal Experiments

To further estimate the roles of HSF on immunologic function in vivo, we generated a subcutaneous xenograft mouse model using various mice species. Briefly, a total of 40 C57BL/6 mice and 16 male athymic BALB/c nude mice (5 weeks old) were purchased from LingChang Biotechnology Co., LTD (license number: SCXK (Hu) 2018–0003; Shanghai, China) and SLAC Laboratory Animal Co., Ltd (license number: SCXK (Hu) 2022–0004; Shanghai, China). All mice were adaptively bred for 1 week and housed at 22±1°C and 55% humidity with a 12-h light/12-h dark cycle in the Eyong Pharmaceutical Research and Development Co., LTD (license number: SYXK (Zhe) 2021–0033; Zhejiang, China). For in vivo xenograft experiments, mice were randomly allocated to normal, model, or HSF groups, 8 in each group.[31,32] The size of the sample was established in accordance with previous research and practical considerations, with the goal of achieving adequate statistical power while reducing the number of animals used. All experiments were conducted with independent biological replicates (n= 8 per group), unless stated otherwise. Subsequently, 1×10^6 LLC-Luc cells in 0.1 mL DMEM were subcutaneously injected into the right flank of 6-weeks-old C57BL/6 mice and nude recipients in model and HSF groups, respectively. The researcher responsible for measuring tumor size with calipers was blinded to the group allocation of the mice. After the tumor volume had grown to 100 mm^3, the mice in the HSF group were intragastrically administered using HSF (6 g/kg, refer to our previously published article by Jin et al.[21] Hangzhou KeShi Biotechnology Co., LTD, Zhejiang, China) daily for 15 days. Meanwhile, the normal and model groups were treated with a saline solution daily for 15 days. The individual administering the treatments (eg, drug or vehicle) was not involved in the subsequent measurements. The tumor volume was determined using a caliper every 3 days and calculated using the following formula: Tumor volume (mm^3) = (width) × $(height)^2/2$. Besides, the body weight was measured twice per week. At the end of the experiment, all mice were anesthetized using 4% chloral hydrate (Sigma, St. Louis, MO), then the luciferase signal intensity was examined using BLT AniView100 fluorescence imaging system (Guangzhou Biolight

Biotechnology Co., Ltd, Guangzhou, China). After that, blood was collected from the inner canthus in C57BL/6 mice for further analysis. After euthanized, all tumor tissues from C57BL/6 and nude mice were collected and weighed. Further, the thymus and spleen tissues from C57BL/6 mice were removed and weighed. Finally, the thymus index and spleen index were calculated to assess the immunomodulatory activity in LLC-Luc-bearing mice using the following formula: organ weight/body weight. The initial data analysis (eg, statistical comparisons) was performed using coded group designations to ensure objectivity.

Detection of the Cytokines IFN-γ, IL-2, IL-10, and IL-4 in Serum

Peripheral blood was harvested and then centrifuged at 3,000 rpm for 15 min to obtain the serum. Serum levels of IFN-γ (Enzyme-linked Biotechnology Co., Ltd., Shanghai, China), Interleukin-2 (IL-2), Interleukin-10 (IL-10), and Interleukin-4 (IL-4) were measured by the ELISA kits (Thermo Fisher Scientific Inc), according to manufacturer's instruction.

Histopathology Analysis

The tumor tissues from C57BL/6 mice were immediately fixed in 4% paraformaldehyde for 3 days. After paraffin embedding, tumor tissues were sliced into approximately 4 μm sections. Then, the sections were stained with hematoxylin and eosin and further examined under a light microscope (Nikon Eclipse Ci-L, Japan).

Cell Transfection

The hU6-MCS-CMV-Puromycin lentiviral vectors (GV112) and short hairpin RNA (shRNA) for IL-10 were obtained from GeneChem Co Ltd. (Shanghai, China). shRNA targeting IL-10 was cloned into lentiviral vectors based on the manufacturer's protocols. Furthermore, lentivirus was transfected into LLC cells, and puromycin was used to select the infected cells. Subsequently, the knockdown efficiencies were verified by quantitative real-time polymerase chain reaction (QRT-PCR) and Western blot assays.

Tumor Xenograft Experiment

To estimate the effects of HSF on tumor growth in LLC with IL-10 knockdown, additional 16 C57BL/6 mice were used to perform the tumor xenograft experiment. Mice were divided randomly into the $LLC^{IL-10-/-}$ and $HSF+LLC^{IL-10-/-}$ groups (n=8 in each group). Then, LLC cells with IL-10 knockdown were subcutaneously injected into C57BL/6 mice. Also, mice in the $HSF+LLC^{IL-10-/-}$ group received administrations with 6 g/kg of HSF once a day for 15 days. The tumor size was measured every 3 days, and then tumor tissue was removed and weighed after 15 days for immune cell cluster analysis.

Flow Cytometry Analysis

Tumor tissues from HSF-treated C57BL/6 mice with or without IL-10 knockdown were immersed in DMEM with 1% FBS, cut with a knife, and processed through a 70-m nylon membrane to yield single-cell preparations. Then, cells were placed on ice in FACS buffer for 30 min of staining with the following surface antibodies: F4/80 (1:500 dilution, F21480A02, MultiSciences, Hangzhou, China), CD11b (1:1000 dilution, F11011B03, MultiSciences), CD25 (1:200 dilution, F2102503, MultiSciences), CD127 (1:200 dilution, F2112702, MultiSciences), CD3 (1:200 dilution, AM003E0205-100, MultiSciences), CD4 (1:1000 dilution, SC-19641PERCP, Santa), CD8 (1:200 dilution, AM008A0204-100, MultiSciences), CD44 (1:200 dilution, F1104403, MultiSciences), and CD62L (1:500 dilution, 746726, BD Biosciences) for 1 h at room temperature. Following two washes with the flow cytometry staining buffer, cells were discriminated by blinded investigators using a NovoCyte flow cytometry (Agilent, USA) and analyzed with FlowJo 10.6.1 (BD Biosciences, USA).

Isolation of $CD8^+$ T Cells by Magnetic Bead Cell Sorting

$CD8^+$ T cells were isolated from spleen tissues in C57/BL mice using magnetic bead cell sorting. The splenocytes were labeled with primary CD8 antibody (MultiSciences, Hangzhou, China) followed by incubation with anti-mouse IgG microbeads according to the manufacturer's instructions. Next, the magnetic bead cell sorting was conducted using the

mouse $CD8^+$ T cell enrichment kit (StemCell Technologies). To obtain great purity, we repeated a positive choice with an LS column three times. $CD8^+$ T cells were used for proliferation, apoptosis, and functional assays.

Apoptosis Assay

Annexin V apoptosis detection kit (#556547, BD Biosciences, USA) was used for the analysis of apoptosis. In short, $CD8^+$ T cells were seeded in 6-well plates at a density of 2×10^5/mL and then treated with 0.2 mg/mL of HSF or HSF +aqueous buffer containing 0.1% BSA or HSF+IL-10 (2 ng/mL, P5165, Beyotime) for 24 h. Next, the cells were trypsinized, collected, and resuspended. Approximately 1×10^5 cells were harvested and resuspended in 500 mL binding buffer, followed by staining with 5 μL 1× Annexin V-FITC and 10 μL propidium iodide (PI) for 15 min in dark at room temperature. Finally, the cells were analyzed by a flow cytometer and FlowJo software.

CFSE Staining Assay

CFSE staining assay was conducted to assess the proliferative capacity of $CD8^+$ T cells. Briefly, $CD8^+$ T cells were washed and resuspended with DMEM and then seeded in the 96 well plates at a final concentration of 1×10^6 cells/mL. $CD8^+$ T cells were stained with 5 Mm of carboxy-fluorescein succinimidyl ester (CFSE, C1031, Beyotime) for 15 min at 37°C. Subsequently, the staining reaction was stopped with DMEM with 10% FBS. CFSE-labeled $CD8^+$ T cells were washed with a complete medium and seeded (1×10^5 cells/well) into 24-well plates, and then HSF (0.2 mg/mL) or HSF +IL-10 was added to the medium. After treatment as indicated for 3 days, cell proliferation of $CD8^+$ T cells was analyzed by flow cytometry.

Detection of the Granzyme B and IFN-γ in $CD8^+$ T Cells

$CD8^+$ T cells (1×10^5) were placed in the 24-well plates coated with CD3/CD28 antibodies and HSF or HSF+IL-10 treated for 3 days. Next, the $CD8^+$ T cells were treated with 40 ng/mL of PMA, 250 ng/mL of Ionomycin, and 5 μg/mL Golgi plug (Brefeldin A) for 4 h at 37 °C with 5% CO_2. After that, the $CD8^+$ T cells were collected and ruptured with Cytofix/Cytoperm (BD Bioscience) for 30 min at 4 °C. After washing twice with permeabilization wash buffer, the $CD8^+$ T cells were exposed to granzyme B (GZMB) and interferon-γ (IFN-γ) antibodies for 30 min at 4 °C. Further, the $CD8^+$ T cells were resuspended in 200 μL FACS buffer solution for FACS examination.

Analysis of Cell Origin of IL-10 in Tumor Tissues From HSF-Treated Mice

A suitable amount of single-cell suspension prepared from tumor tissues in the HSF-treated group was incubated with cell surface fluorescence-conjugated antibodies (immune cells: CD45 (1:200, F2104501, MultiSciences); CD4 T cells: CD4, CD8; B cells: B220 (1:500, #563103, BD); myeloid-derived suppressor cells (MDSCs): CD11b, Gr-1 (1:200, #553124, BD) for 30 minutes before being flow cytometrically analyzed. The data were statistically analyzed using FlowJo 7.6 software.

Real-Time Quantitative PCR (RT-qPCR)

Total RNA from tumor tissues and LLC cells was extracted using an EZ-10 Total RNA Mini-Preps kit (Sangon Biotech (Shanghai) Co., Ltd, China), and cDNA synthesis was carried out using a reverse transcription kit (JiangSu CoWin Biotech Co., Ltd, China) following the manufacturer's manuals. Immediately afterwards, the qRT-PCR was conducted using an SYBR Green Master Mix Kit (Yeasen Biotechnology (Shanghai) Co., Ltd, China) through PCR LightCycler® 96 (Roche Diagnostics, Basel, Switzerland). The primer sequences used for qPCR were as follows: IFN-γ forward, 5′-GCCACGGCACAGTCATTGA-3′; reverse, 5′-TGCTGATGGCCTGATTGTCTT-3′; IL-2 forward, 5′-TGAGCAGGATGGAGAATTACAGG-3′; reverse, 5′-GTCCAAGTTCATCTTCTAGGCAC-3′; IL-4 forward, 5′-GGTCTCAACCCCCAGCTAGT-3′; reverse, 5′-GCCGATGATCTCTCTCAAGTGAT-3′; IL-10 forward, 5′-CTTACTGACTGGCATGAGGATCA-3′; reverse, 5′-GCAGCTCTAGGAGCATGTGG-3′; IL-10R forward, 5′-TTGTCGCGTTTGCTCCCATT-3′; reverse, 5′-GAAGGGCTTGGCAGTTCTG-3′, and β-actin forward, 5′-GTGACGTTGACATCCGTAAAGA-3′; reverse, 5′-GCCGGACTCATCGTACTCC-3′. Finally, the relative gene expression level was quantified using the $2^{-\Delta\Delta Ct}$ method.[33]

Western Blot

Total protein from tumor tissues, LLC, and $CD8^+$ T cells was extracted using RIPA buffer (P0013B, Beyotime Biotech, Shanghai, China) and quantified using a BCA protein assay kit (pc0020, Solarbio). Shortly afterwards, the total protein was separated in sodium dodecyl sulfate-polyacrylamide gel electrophoresis (SDS-PAGE) and transferred to a PVDF membrane (IPVH00010, Millipore). After blocking with 5% skimmed milk for 1.5 h, the membranes were incubated with anti-IL-10R (1:1000, ab225820, Abcam, Cambridge, UK), anti-p-STAT3 (1:1000, AF3293, Affinity), anti-STAT3 (1:1000, AF6294, Affinity), anti-p-STAT1 (1:1000, AF3300, Affinity), STAT1 (1:1000, AF6300, Affinity), anti-IL-10 (1:1000, bs-6761R, BEIJING BIOSYNTHESIS BIOTECHNOLOGY CO., LTD. China), and anti-β-actin (1:10000, AF7018, Affinity) overnight at 4 °C. Subsequently, the membranes were incubated with HRP-linked secondary antibodies for 2 h at room temperature. At last, the protein bands were visualized using enhanced chemiluminescence (ECL) kit (Beyotime, China) and assessed using Image J software (v1.46, National Institutes of Health, Bethesda, MD, USA).

Statistical Analysis

Data were presented as mean ± standard deviation. The normality (assessed using the Shapiro–Wilk test) and the homogeneity of variance (evaluated through the Brown-Forsythe test) were initially examined. The significance of differences was analysed using one-way analysis of variance (ANOVA) with Tukey's post hoc test between multiple groups. And, the comparisons between the two groups were conducted using Student's *t-tests*. All statistical analyses were performed using the SPSS 21.0 (SPSS, Inc., Chicago, IL, USA). Statistical significance was deemed when $P < 0.05$.

Results

Effect of HSF on Tumor Growth and Immunologic Function in LLC-Luc Bearing Mice

As illustrated in Figure 1, the tumor volume and tumor weight were significantly decreased in the HSF-treated group when compared with the model group in C57BL/6 mice (Figure 1A–C), while there was no obvious difference between the HSF-treated group and model group in nude mice (Figure 1B–D). These findings were supported by in vivo imaging techniques (Figure 1A). Furthermore, we found that HSF treatment significantly increased the thymus index and spleen index compared with that in the model group (Figure 2A and B). In addition, we evaluated the effect of HSF on histopathological changes in the tumor tissues of C57BL/6 mice. H&E staining indicated that HSF treatment significantly promoted the death of tumor cells in vivo (Figure 2C). Since innate to adaptive immunity plays a critical role in the anti-tumor effects of HSF, we also measured the expression of the secreted cytokines. As a result, HSF treatment indeed induced the increased expression levels of IFN-γ and IL-2, as well as decreased the expression of IL-4, IL-10, and IL-10R in serum samples and tumor tissues compared with the models (Figure 2D and E). IL-10 has been demonstrated to activate the downstream STAT3/STAT1 signaling molecules, accelerate IFN-γ cytokine production, induce the expression of MHC molecules in antigen-presenting cell (APC), and improve effector $CD8^+$ T cell activity by directly connecting to the $CD8^+$ T cell receptor, IL-10R.[34,35] To explore whether HSF mediated immunological reaction via the STAT pathway, Western blotting was employed to evaluate protein levels of STAT3 and STAT1 and their phosphorylation level. As shown in Figure 2F, treatment of HSF significantly decreased the protein levels of IL-10R, p-STAT3, and p-STAT1 in tumor tissues.

Effect of HSF on T Cells Population in the Tumor Microenvironment

To investigate the effect of HSF on the immune cell distribution in TME, we recognized the infiltration of macrophages and T cells in tumor tissue by flow cytometry. Compared with the model group, we found that tumor-associated macrophages (TAMs) displayed as $CD45^+CD11b^+F4/80^+$ population and regulatory T cells displayed as $CD4^+CD25^+CD127^-$ population were significantly decreased in HSF group (Figure 3A and B). Additionally, HSF also obviously contributed to $CD4^+$ and $CD8^+$ T cell infiltration in tumor tissues (Figure 3C and D). For T cell subsets, HSF noticeably increased the percentage of $CD44^{Low}CD62L^{High}$ Naïve T cells and $CD44^{High}$ $CD62L^{High}$ central memory T cells (T(CM)) to $CD4^+$ T cell populations in the tumor tissues of C57BL/6 mice (Figures 3E), and also significantly

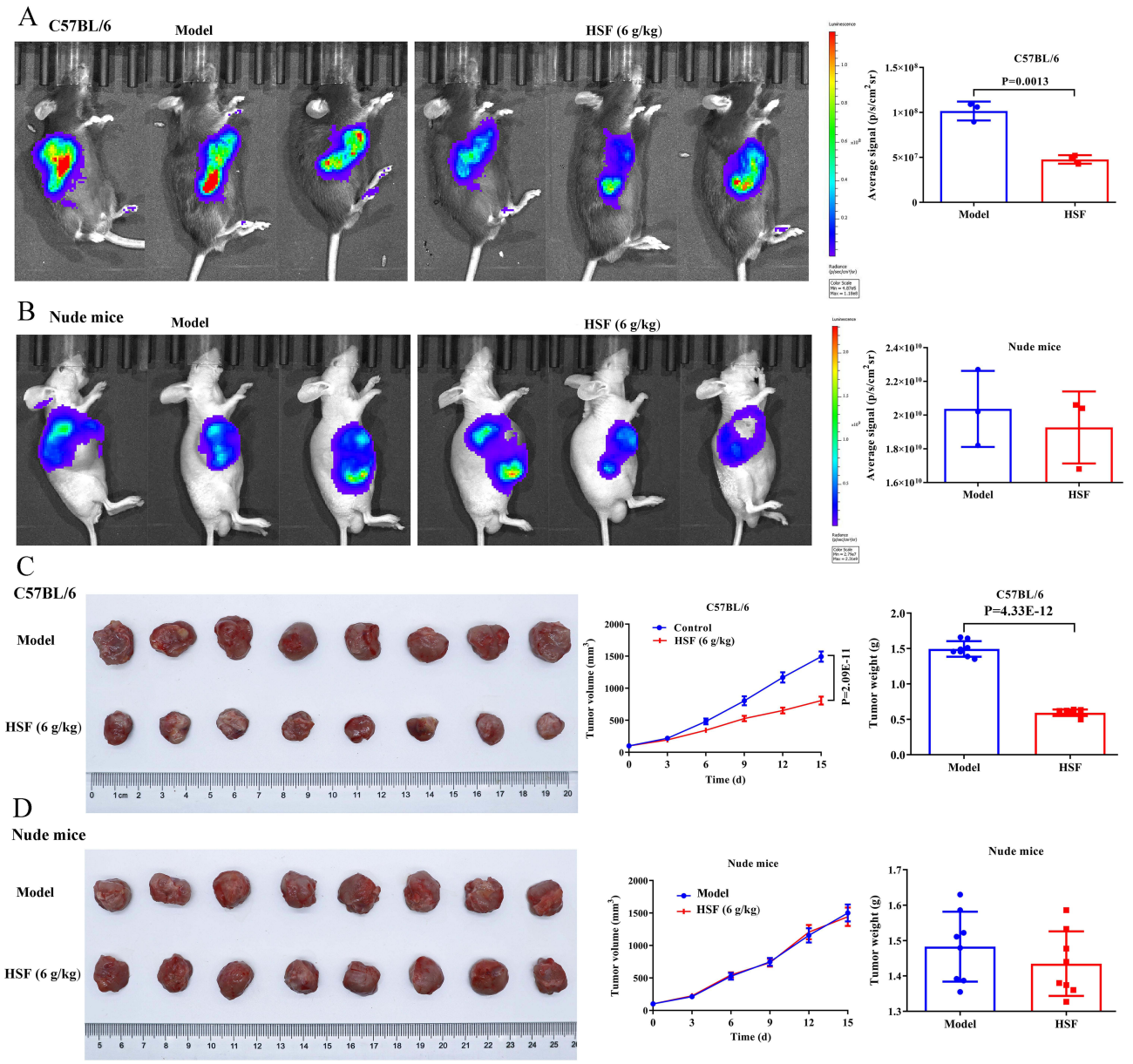

Figure 1 HSF suppresses tumor growth in C57BL/6 mice bearing Lewis lung cancer (LLC)-Luc. Representative luciferase images of (**A**) LLC-Luc bearing C57BL/6 mice and (**B**) nude mice. Three mice from each group selected for exhibition. (**C** and **D**) Image of xenograft tumors, tumor growth curves and, tumor weights in C57BL/6 mice and nude mice subcutaneously injected with the LLC-Luc cells (n=8). Data were presented as each dot for one animal and the exact p shown on plot.

increased the proportion of $CD44^{Low}CD62L^{High}$ and $CD44^{High}CD62L^{High}$ to $CD8^{+}$ T cell populations (Figure 3F). In general, these data indicated that immunomodulatory properties might help in the anti-NSCLC effects of HSF.

Effect of HSF on Tumor Growth and T Cells Population in IL-10 Knock-Down of LLC-Bearing Mice

To further illustrate the immunomodulatory properties of IL-10, another xenograft mouse model was used to confirm the effect of HSF on tumorigenesis in IL-10 knock-down of LLC-bearing mice. LLC cells transfected with sh-IL-10 or sh-NC lentiviral were subcutaneously inoculated into male C57BL/6 mice. The expression of IL-10 was determined using qRT-PCR and Western blot assays. Results showed that in the sh-IL-10 group, the mRNA and protein expression levels of IL-10 were significantly down-regulated (Figure 4A and B). Moreover, it has shown that the tumor volume, tumor weight, and the protein expression levels of IL-10R, p-STAT3, STAT3, p-STAT1, and STAT1 in $HSF+LLC^{IL-10-/-}$ group have no statistically significant

https://doi.org/10.2147/DDDT.S531106

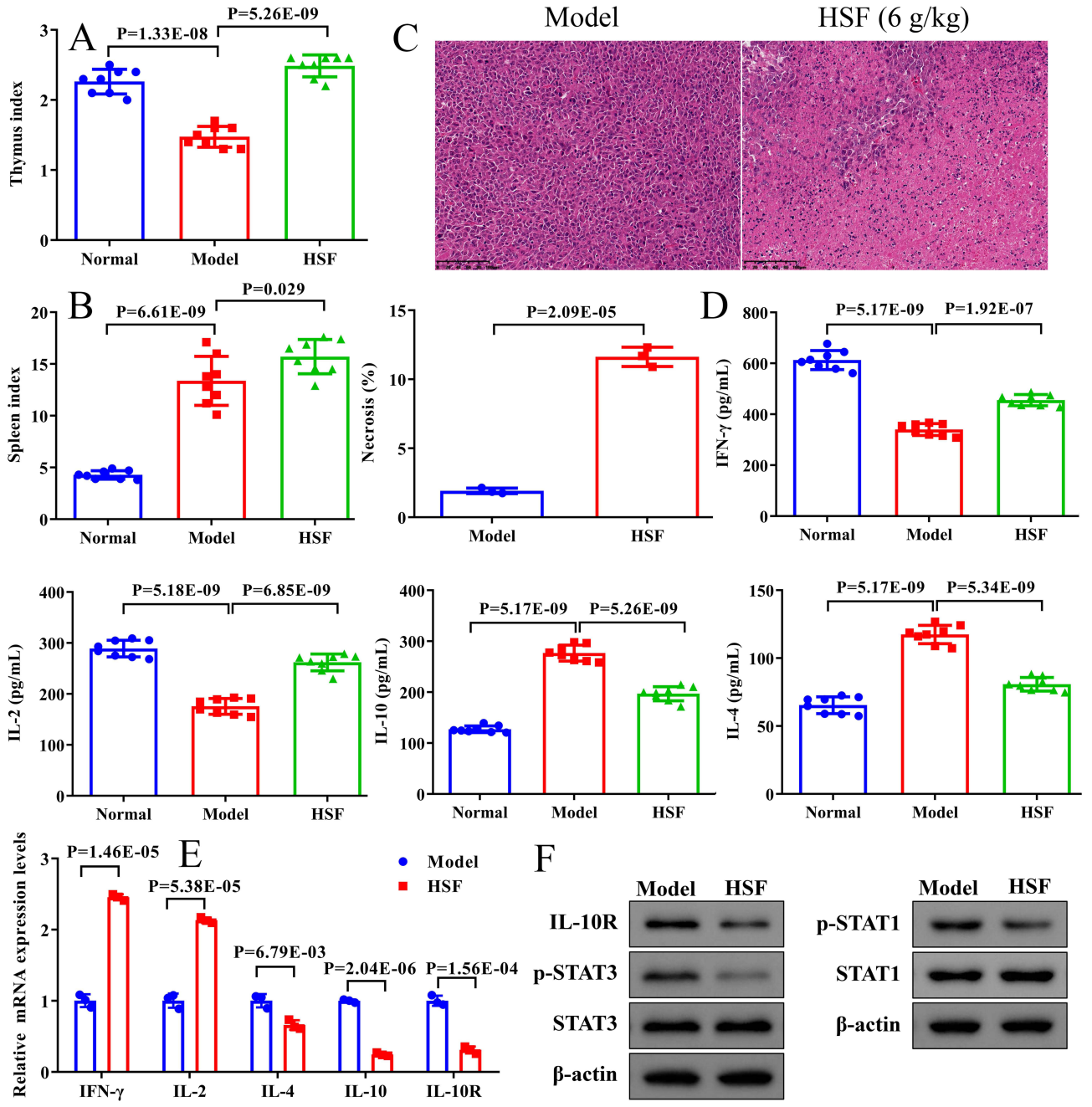

Figure 2 HSF ameliorates immunologic function in LLC-Luc allograft C57BL/6 mice. Effect of HSF on the thymus index (**A**) and spleen index (**B**) of HSF-treated tumor-bearing C57BL/6 mice (n=8). (**C**) Histological analysis for tumor tissues by H&E staining (n=8). (**D**) Effect of HSF on the levels of IFN-γ, IL-2, IL-10, and IL-4 cytokine in the serum detected by ELISA (n=8). (**E**) Effect of HSF on the mRNA expression levels of IFN-γ, IL-2, IL-4, IL-10, and IL-10R detected by qRT-PCR assay (n=8). (**F**) Effect of HSF on the protein expressions of IL-10R, p-STAT3, STAT3, p-STAT1, and STAT1 in tumor tissues detected by Western blot. Data were showed as each dot for one animal and the exact p shown on plot.

differences when compared with the LLC$^{IL-10-/-}$ group (Figure 4C and D). Most importantly, results of flow cytometry assay showed that HSF substantially decreased TAMs and population and regulatory T cells, increased CD4$^+$ T cells infiltration as well as Naïve T cells and T(CM) to CD4$^+$ T cell populations in tumor tissues, while the CD8$^+$ T cells infiltration and Naïve T cells and T(CM) to CD8$^+$ T cell populations with no change occurred in IL-10 knock-down of LLC bearing mice (Figure 5A–F).

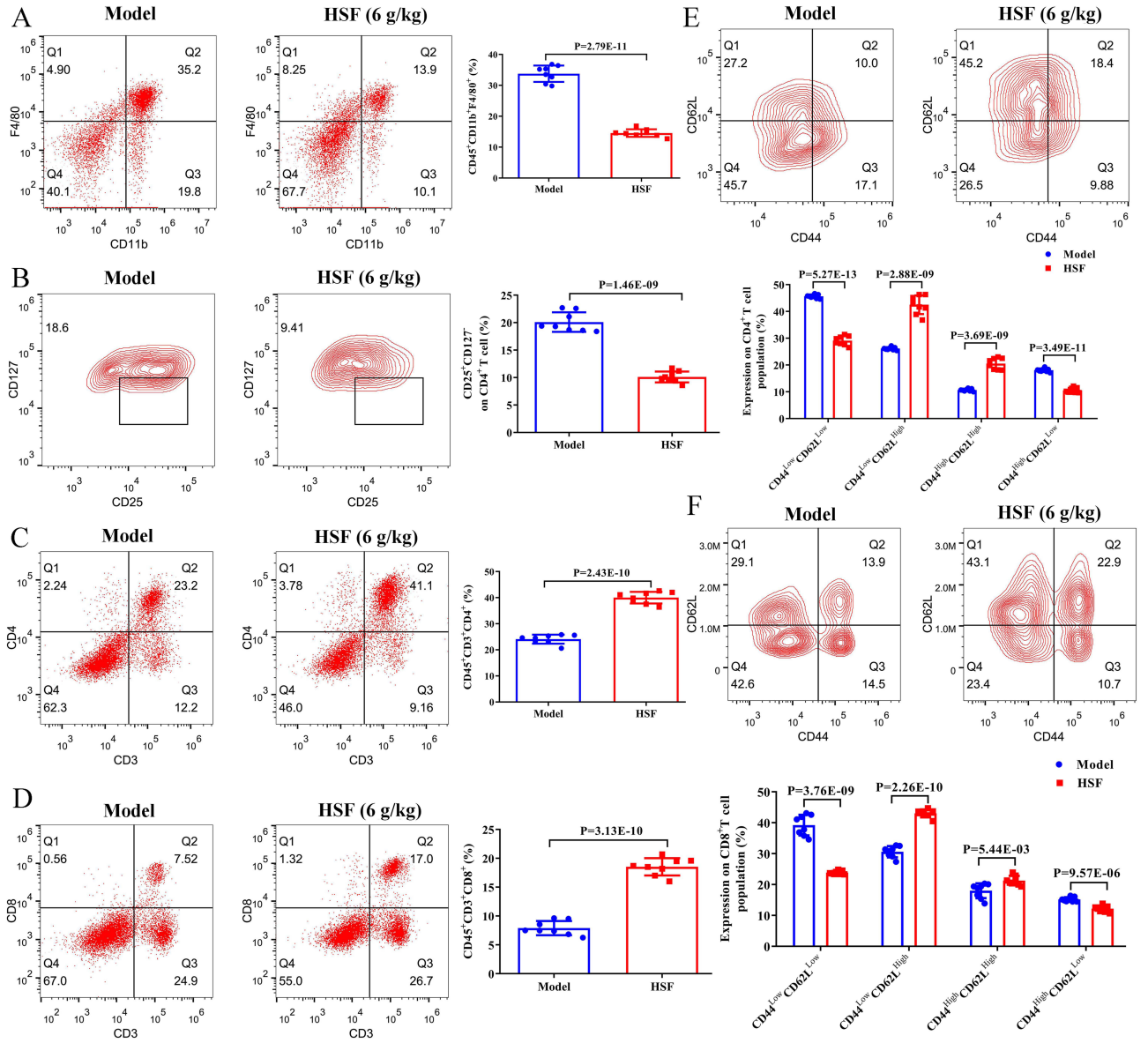

Figure 3 HSF decreased TAMs and regulatory T cells and increased memory T cells population in the tumor microenvironment. (**A**) Percentage of TAMs (displayed by $CD11b^{+}F4/80^{+}$ staining) in tumor tissue. (**B**) Percentage of regulatory T cells (displayed by $CD25^{+}CD127^{-}$ staining) in tumor tissue. (**C**) Percentage of $CD4^{+}$ T cells (displayed by $CD3^{+}CD4^{+}$ staining) in tumor tissue. (**D**) Percentage of $CD8^{+}$ T cells (displayed by $CD3^{+}CD8^{+}$ staining) in tumor tissue. Percentage of T(CM) (displayed by $CD44^{High}CD62L^{High}$ staining) and Naïve T cells (displayed by $CD44^{Low}CD62L^{High}$ staining) of (**E**) $CD4^{+}$ and (**F**) $CD8^{+}$ T cells in tumor tissue. Data were presented as each dot for one animal and the exact p shown on plot.

Effect of HSF on Cell Apoptosis, Proliferation, and Function of $CD8^{+}$ T Cells in vitro

In this study, $CD8^{+}$ T cells were isolated from the spleen tissues of C57BL/6 mice and incubated with HSF or HSF+IL-10 for 24 h. Results showed that HSF significantly promoted cell proliferation and attenuated cell apoptosis of $CD8^{+}$ T cells (Figure 6A and B). Release of GzmB and IFN-γ is one of the important mechanisms of $CD8^{+}$ cytotoxic T cells to destroy tumor cells.[36,37] In the subsequent study, we found that HSF significantly increased the expression levels of GzmB and IFN-γ compared to the control group (Figure 6C). Also, the Western blot results revealed that $CD8^{+}$ T cells after treatment with HSF had lower protein levels of IL-10R, p-STAT3, and p-STAT1 (Figure 7A). Meanwhile, the effects of HSF on cell apoptosis, proliferation, function, and STAT3/STAT1 pathway of $CD8^{+}$ T cells were counteracted under IL-10 treatment (Figure 6 and 7A). To sum up, these data suggested that HSF regulated $CD8^{+}$ T cells affect tumor growth and T cells population by modulating IL-10, and may have influences on STAT3/STAT1 signaling pathway.

https://doi.org/10.2147/DDDT.S531106

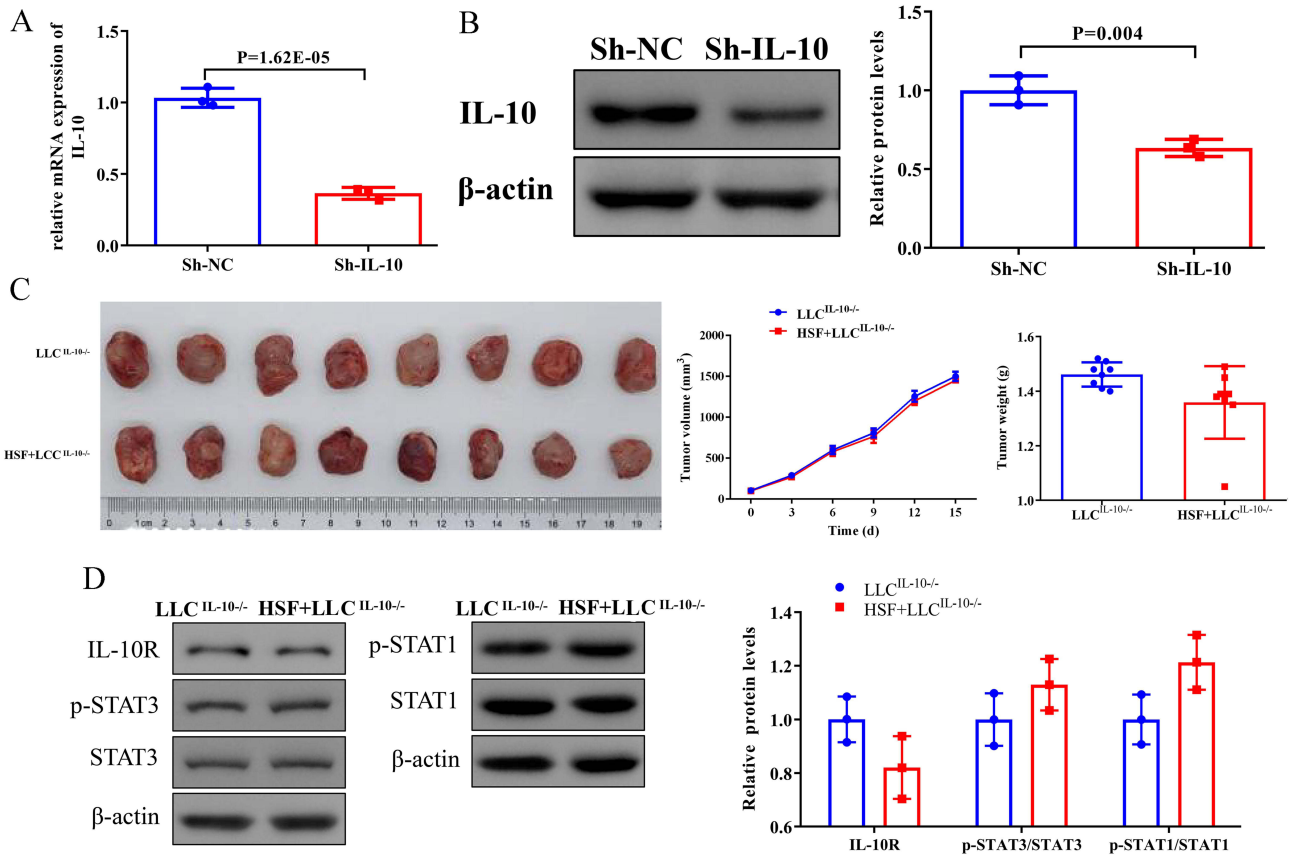

Figure 4 HSF failed to inhibit tumor growth in C57BL/6 mice bearing IL-10 knockdown of LLC. (**A** and **B**) IL-10 expression in LLC cells transduced with sh-IL-10 and normal control (NC) was detected by qRT-PCR and Western blotting. (**C**) Image of xenograft tumors, tumor growth curves, and tumor weights in C57BL/6 mice subcutaneously injected with the LLC cells with knockdown of IL-10 (n=8). (**D**) Western blot assay revealed that IL-10R, p-STAT3, STAT3, p-STAT1, and STAT1 protein expression has no significant difference in HSF+LLC$^{IL-10-/-}$ group compared with LLC$^{IL-10-/-}$ group. Data were displayed as each dot for one animal and the exact p shown on plot.

IL-10 in Tumor Tissue of HSF Group Mainly Originated From B Cells

To further determine the cells that primarily generate IL-10 in tumor tissue in the HSF group, flow cytometry was utilized to look at the expression of IL-10 in CD45 $^{+}$ and CD45^{-} cells in the tumor tissues. As shown in Figure 7B, IL-10 in tumor tissues is mostly produced by immunological cells. Additionally, we used flow cytometry to examine the infiltration of B cells, T cells, and MDSCs, as well as the expression level of IL-10, to better understand where IL-10 originates from. The flow cytometry results revealed that B cells had the highest infiltration, followed by CD8^{+} T cells and MDSCs, and the most abundant IL-10-expressing cells were B cells, followed by CD8^{+} T cells and MDSCs (Figure 7C). Altogether, these findings showed that HSF might decrease the production of IL-10 that mainly originated from B cells in tumor tissues.

Discussion

Although the existence of predictive markers for immunotherapy efficacy is not entirely clear, the increased efficacy seen in some patients suggests that the investigation of immunotherapy for lung cancer is essential to further improving patient prognosis. A priceless human legacy that has existed in Asia for more than 3,000 years in traditional Chinese medicine. Herbal remedies are frequently employed in the treatment of complex disorders and have gradually gained recognition as a viable alternative to conventional medications.[38] HSF is an artificial substitute for *Cordyceps sinensis* and has shown promising therapeutic effects in cancer, with its documented bioactive components (eg, polysaccharides, cordycepin), could function as a beneficial adjunct to immune checkpoint inhibitors (ICIs). We suggest that its potential to modulate innate and adaptive immunity-such as promoting dendritic cell maturation, macrophage polarization, or enhancing NK

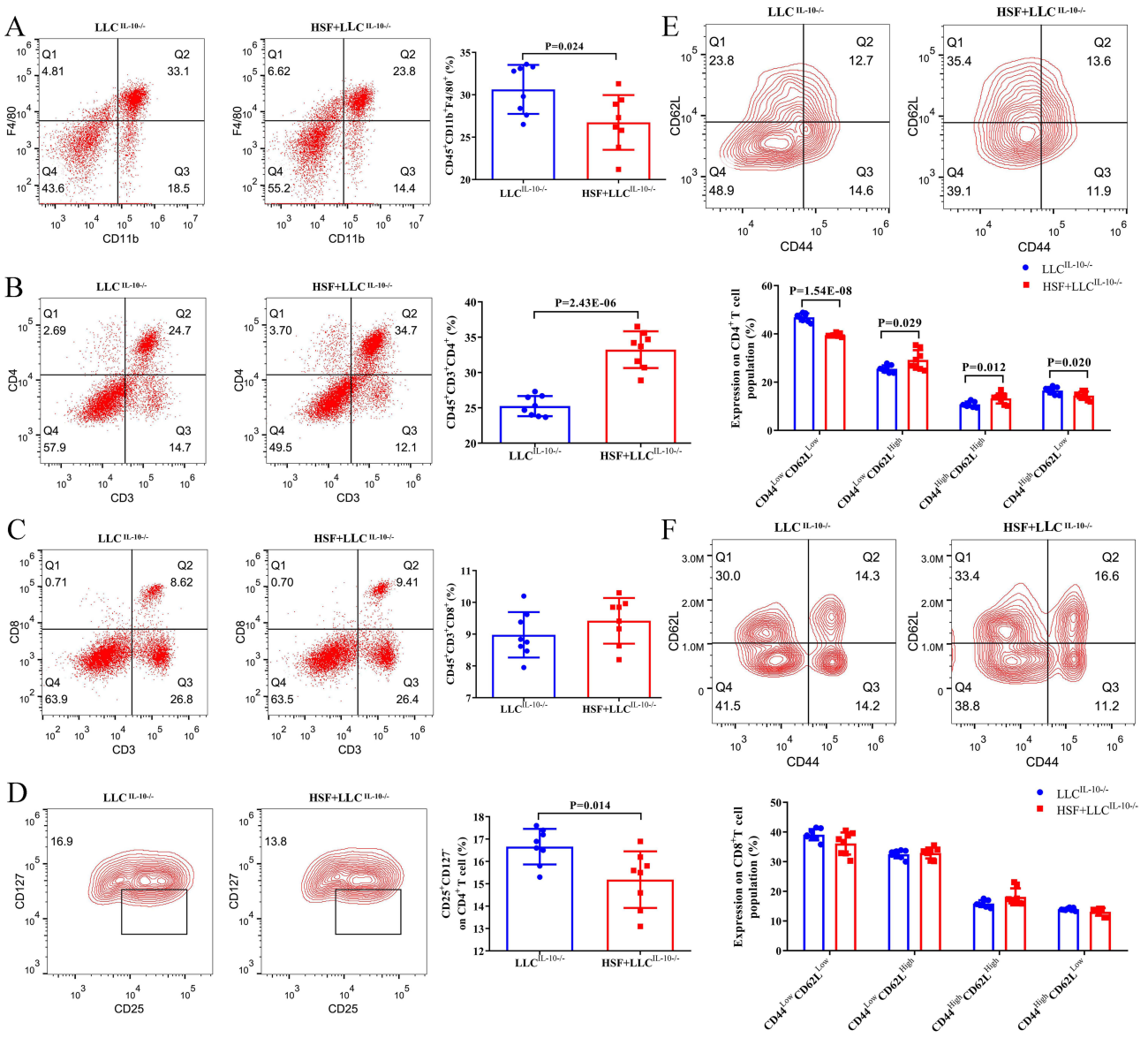

Figure 5 HSF failed to increase memory T cells population in IL-10 knockdown of LLC-bearing mice. (**A**) Percentage of TAMs (displayed by CD11b+F4/80+ staining) in xenograft tumors of IL-10 knockdown LLC bearing mice. (**B**) Percentage of $CD4^+$ T cells (displayed by $CD3^+CD4^+$ staining) in xenograft tumors of IL-10 knockdown LLC bearing mice. (**C**) Percentage of $CD8^+$ T cells (displayed by $CD3^+CD8^+$ staining) in xenograft tumors of IL-10 knockdown LLC bearing mice. (**D**) Percentage of regulatory T cells (displayed by $CD25^+CD127^-$ staining) in xenograft tumors of IL-10 knockdown LLC bearing mice. Percentage of T(CM) (displayed by $CD44^{High}CD62L^{High}$ staining) and Naïve T cells (displayed by $CD44^{Low}CD62L^{High}$ staining) of (**E**) $CD4^+$ and (**F**) $CD8^+$ T cells in xenograft tumors of IL-10 knockdown LLC bearing mice. Data were displayed as each dot for one animal and the exact p shown on plot (n=8).

cell activity-could help convert an immunosuppressive "cold" tumor microenvironment into a more immunogenic "hot" one. This would potentially sensitize NSCLC tumors to subsequent ICI treatment, leading to improved response rates. In this study, we found that HSF inhibited tumor growth in LLC-Luc-bearing C57BL/6 mice. These outcomes are in line with our prior research, which demonstrated that HSF had anti-tumor effects on pulmonary metastasis in breast cancer.[21] Similarly, we also unexpectedly found that HSF has no impact on nude mice. Hence, we hypothesized that HSF could effectively stop the evolution of NSCLC by restoring the system's immune response.

It is well-recognized that the tumor microenvironment plays a crucial role in the growth and spread of tumors. A number of non-malignant cells, such as immune cells, endothelial cells, and macrophages, are known to infiltrate the TME. These non-malignant cells release cytokines and extracellular matrix, which are crucial elements of the TME.[39] One important element of the TME is the tumor-associated macrophage (TAM) population, which influences the

https://doi.org/10.2147/DDDT.S531106

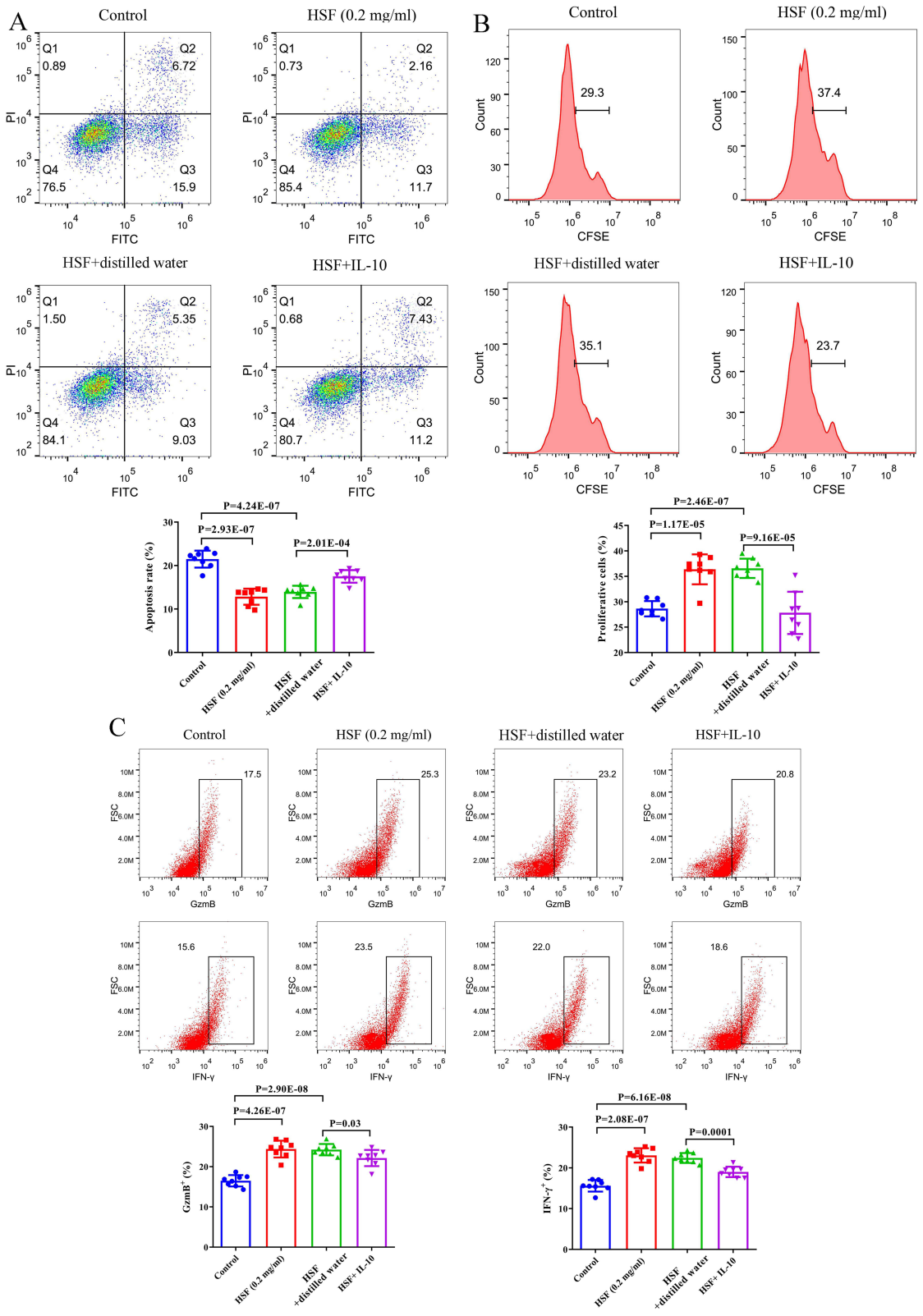

Figure 6 HSF promotes the proliferation, and function of CD8$^+$ T cells, and inhibits apoptosis in vitro. (**A**) Representative flow cytometry results showing that the effects of HSF and HSF combined IL-10 on cell apoptosis in the CD8$^+$ T cells. (**B**) Representative image of flow cytometry and statistical analysis evaluating cell proliferation. (**C**) Flow cytometry of GzmB and IFN-γ percentage in CD8$^+$ T cells after HSF or HSF combined IL-10 treatment. Data were displayed as each dot with exact p value (n=8).

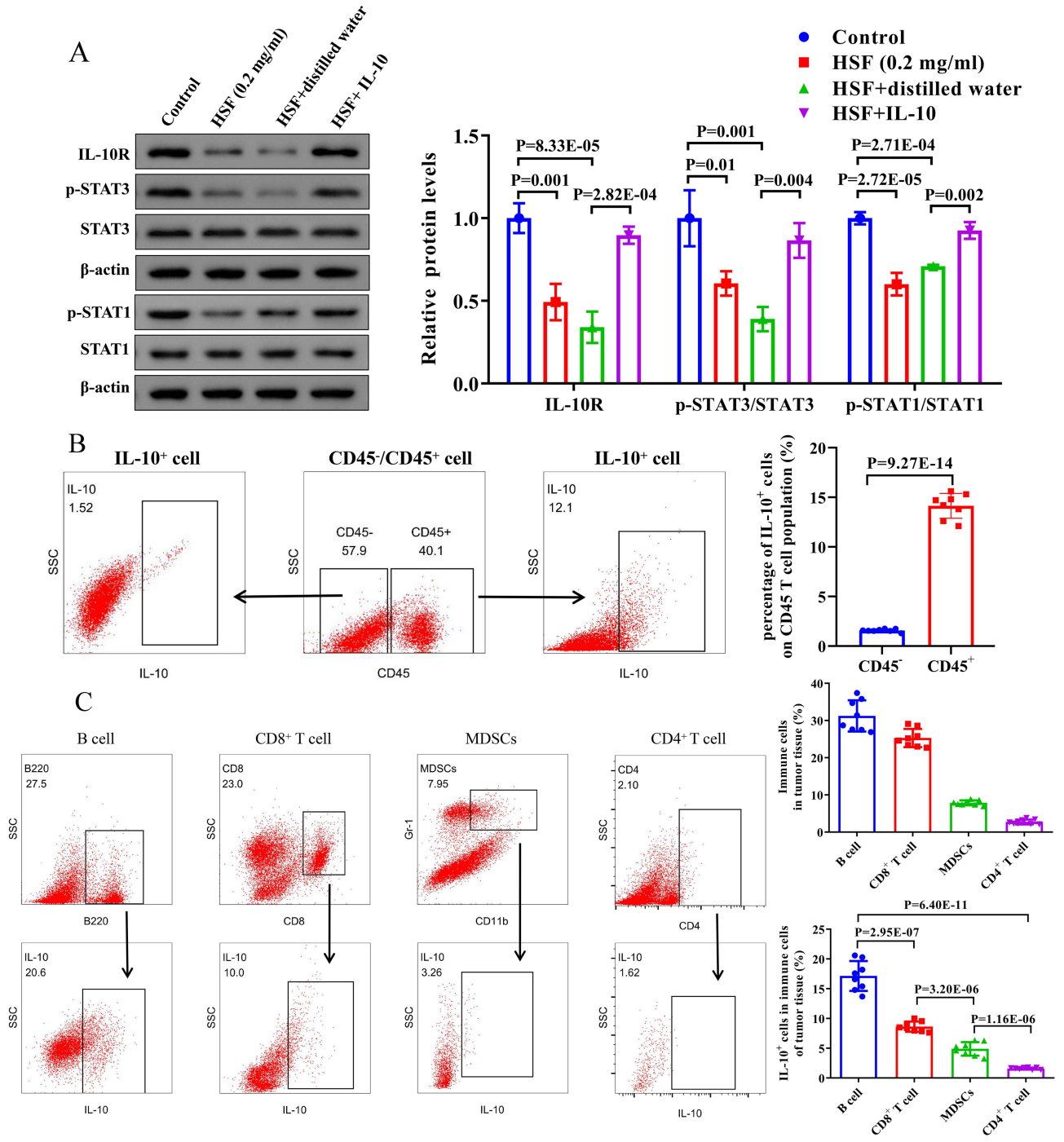

Figure 7 The abundance of B cells, T cells, and MDSCs and their levels of IL-10 expression in tumor tissues of LLC mice. (**A**) The expression of the IL-10R, p-STAT3, STAT3, p-STAT1, and STAT1 was detected by Western blotting after HSF or HSF combined IL-10 treatment. (**B**) Representative flow cytometry results of $CD45^+$ cells and $CD45^-$ cells and statistical analysis of IL-10 percentage on $CD45^+$ cells and $CD45^-$ T cell population of tumor tissues in the HSF-treated group (n=8). (**C**) flow cytometry analysis of B cell, CD8 T cell, MDSCs, and CD4 T cell abundance and corresponding IL-10 levels (n=8). Data were displayed as each dot with exact p value.

malignancy and development of different tumors by the release of cytokines from the tumor.[40] In the tumor microenvironment, $CD25^+CD127^-$ regulatory T cells (Treg) are crucial for dampening anti-tumor immunity. The proportion of Treg is significantly higher in peripheral blood and the local tumor microenvironment of lung cancer patients, and the higher the proportion of Treg in a patient's body, the worse their prognosis.[41] This is the primary cause of tumor immune escape and the challenge in achieving the desired immunotherapy effect. One of the most crucial functional subgroups of

https://doi.org/10.2147/DDDT.S531106

the human immune system, $CD4^+$ cells perform a number of functions, such as helper immunity, cytotoxicity, and cytokine control. Additionally, by secreting cytokines like IL-10 and IL-2, they can have an immunomodulatory role by assisting $CD8^+$ cells in cellular immunity to attack and eliminate tumor cells.[42] $CD8^+$ T cells are essential for antitumor immune system reactions that effectively destroy cancer cells. Three main subgroups of $CD8^+$ T lymphocytes in mice were identified using CD44 and CD62L (L-selectin) surface markers: Naïve T cells (also known as P1; $CD44^{low}CD62L^{high}$), T(CM) (P2; $CD44^{high}CD62L^{high}$), and effector/memory (P3; $CD44^{high}CD62L^{low}$). In naive mice, the residual $CD44^{low}CD62L^{low}$ (P4) $CD8^+$ T cell fraction is a relatively small population that has undergone very little research.[43] In the current study, we found that HSF enhanced the population of $CD4^+$ and $CD8^+$ T cells, as increased the proportion of $CD44^{Low}CD62L^{High}$ and $CD44^{High}CD62L^{High}$ on T cells was increased by the treatment of HSF.

In the TME, IL-10 is the primary activator of STAT3.[44] And, the STAT3 controls the development of $CD8^+$ T cells in malignancy.[45] Naing et al reported that direct IL-10 injection into tumors caused high levels of cytokines to rise, including IFN-γ, IL-4, and IL-18; IFN-γ also upregulated the major histocompatibility complex-I (MHC-I) in tumors and dendritic cells, which increased the anti-tumor cytotoxicity of $CD8^+$ T cells.[46] However, preliminary evidence indicates that IL-10 may play an unexpected protective role in cancer. Various factors could account for the differences observed among these studies, such as the specific cell type that IL-10 targets in various tumors (for instance, myeloid cells versus T cells), or the variations in T cell responses to IL-10 at different stages of effector function.[23] Unlike anti-IL-10 antibodies, in this study, HSF modulates broader immune components. As a result, we demonstrated that HSF could attenuate the inhibition of IFN-γ and IL-2, and the increase of IL-10, as well as the protein expression levels of p-STAT3 and p-STAT1 in LLC-Luc-bearing C57BL/6 mice. Moreover, the depletion of IL-10 in LLC cells completely abolished the anti-tumor growth, immune regulation effects, and down-regulation of the STAT3/STAT1 signaling pathway induced by HSF. Taken together, these results indicated that HSF could inhibit tumor growth and promote infiltration of $CD8^+$ T cells may indirectly modulate the IL-10/STAT3/STAT1 signaling pathway.

It has been shown that strengthening $CD8^+$ T cells in vitro culture systems can increase the anti-tumor activities of these cells by extending their survival duration and enhancing their function in vivo.[47] In comparison to effector memory $CD8^+$ T cells, stem-cell memory $CD8^+$ T cells and central memory $CD8^+$ T cells have a better ability for self-renewal and are capable of producing an immune response that is both quicker and more intense.[48] Activated $CD8^+$ T lymphocytes can also mediate tumor cell lysis by secreting perforins, granzymes, and cytokines, which cause tumor cells to be destroyed.[49,50] Therefore, increasing $CD8^+$ T cell function is currently focused on promoting $CD8^+$ T cell memory differentiation, extending the lifespan of stem-cell memory $CD8^+$ T cells and central memory $CD8^+$ T cell subset, promoting killing function, and lowering apoptosis. Interestingly, our previous research showed that HSF facilitated the polarization of macrophages towards the M1 phenotype and stimulated $CD8^+$ T cell activation through CCRL2, which in turn impeded the advancement of lung cancer.[51] Similarly, this study revealed that treatment of HSF was found to promote the proliferation, GzmG, IFN-γ levels, and the inactivation of IL-10/STAT3/STAT1 signaling pathway, as well as suppress apoptosis of $CD8^+$ T cells, whereas HSF+IL-10 treatment had opposite effects. Accumulating studies have implied that IL-10 is primarily produced by immune cells, specifically B Cells and MDSCs, in tumor tissues.[52,53] B cell-derived IL-10 may bridge humoral and cellular immunity in TME. In this research, flow cytometry assays also demonstrated that IL-10 produced by tumor tissues is primarily produced by B cells and $CD8^+$ T cells. These findings suggested that depressing IL-10 produced by B cells and $CD8^+$ T cells may be helpful in the display of immunomodulatory functions of HSF in lung cancer. However, this study has certain limitations. Further studies are needed to determine the long-term effects of HSF. Also, high-throughput analysis on tumor tissues should be performed to explore the other underlying mechanisms of HSF in lung cancer.

Conclusion

In summary, we found that HSF suppressed tumor growth and promoted the proliferation and function of $CD8^+$ T cells by inhibiting IL-10/STAT3/STAT1 signaling pathway, suggesting that HSF might serve as an ideal and novel therapeutic strategy to trigger intratumoral $CD8^+$ T cell effector function and improve the tumor microenvironment in lung cancer by modulating the IL-10 pathway.

Abbreviations

CAR, chimeric antigen receptor; CAR-T, chimeric antigen receptor modified T-cell; DMEM, Dulbecco's modified Eagle's medium; ELISA, Enzyme-linked immunosorbent assay; ECL, enhanced chemiluminescence; HSF, *Hirsutella sinensis fungus*; H&E, hematoxylin and eosin; IFN-γ, Interferon-γ; IL-2, Interleukin-2; IL-10, Interleukin-10; IL-4, Interleukin-4; LLC, Lewis lung cancer; LLC-Luc, LLC luciferase; MDSC, myeloid-derived suppressor cells; MHC, major histocompatibility complex; NSCLC, non-small cell lung cancer; QRT-PCR, quantitative real-time polymerase chain reaction; shRNA, short hairpin RNA; SDS-PAGE, sodium dodecyl sulfate-polyacrylamide gel electrophoresis; TME, tumor microenvironment; TAAs, tumor-associated antigens; TCM, Traditional Chinese medicine; TAMs, tumor-associated macrophages.

Data Sharing Statement

All data that support the findings of this study are available from the corresponding author (Dr. Xinhai Zhu) upon reasonable request.

Ethics Approval

All procedures were approved by the Animal Experimentation Ethics Committee of Zhejiang Eyong Pharmaceutical Research and Development Center (No. ZJEY-20220714-01) and performed in full accordance with China's national standard GB/T 35892-2018 (Guidelines for Ethical Review of Laboratory Animal Welfare) and the ARRIVE guidelines.

Author Contributions

All authors made a significant contribution to the work reported, whether that is in the conception, study design, execution, acquisition of data, analysis and interpretation, or in all these areas; took part in drafting, revising or critically reviewing the article; gave final approval of the version to be published; have agreed on the journal to which the article has been submitted; and agree to be accountable for all aspects of the work.

Funding

This work was supported by Zhejiang Provincial Traditional Chinese Medicine Scientific Research Fund Project (NO. 2021ZA004).

Disclosure

The authors declare that there are no conflicts of interest associated with this work.

References

1. Wang Y, Chen R, Wa Y. et al. Tumor Immune Microenvironment and Immunotherapy in Brain Metastasis From Non-Small Cell Lung Cancer. *Front Immunol*. 2022;13:829451. doi:10.3389/fimmu.2022.829451
2. Lahiri A, Maji A, Potdar PD, et al. Lung cancer immunotherapy: progress, pitfalls, and promises. *Mol Cancer*. 2023;22(1):40. doi:10.1186/s12943-023-01740-y
3. Chen L, Chen F, Li J, et al. CAR-T cell therapy for lung cancer: potential and perspective. *Thorac Cancer*. 2022;13(7):889–899. doi:10.1111/1759-7714.14375
4. Wang H, Kaur G, Sankin AI, Chen F, Guan F, Zang X. Immune checkpoint blockade and CAR-T cell therapy in hematologic malignancies. *J Hematol Oncol*. 2019;12(1):59. doi:10.1186/s13045-019-0746-1
5. Willsmore ZN, Coumbe BGT, Crescioli S, et al. Combined anti-PD-1 and anti-CTLA-4 checkpoint blockade: treatment of melanoma and immune mechanisms of action. *Eur J Immunol*. 2021;51(3):544–556. doi:10.1002/eji.202048747
6. Wang T, Shen Y, Luyten S, Yang Y, Jiang X. Tissue-resident memory CD8+ T cells in cancer immunology and immunotherapy. *Pharmacol Res*. 2020;159:104876. doi:10.1016/j.phrs.2020.104876
7. Mami-Chouaib F, Blanc C, Corgnac S, et al. Resident memory T cells, critical components in tumor immunology. *J Immunother Cancer*. 2018;6(1):87. doi:10.1186/s40425-018-0399-6
8. Zhao H, Teng D, Yang L, et al. Myeloid-derived itaconate suppresses cytotoxic CD8+ T cells and promotes tumour growth. *Nat Metab*. 2022;4(12):1660–1673. doi:10.1038/s42255-022-00676-9
9. Domvri K, Petanidis S, Zarogoulidis P, et al. Treg-dependent immunosuppression triggers effector T cell dysfunction via the STING/ILC2 axis. *Clin Immunol*. 2021;222:108620. doi:10.1016/j.clim.2020.108620

10. Bray F, Laversanne M, Sung H, et al. Global cancer statistics 2022: GLOBOCAN estimates of incidence and mortality worldwide for 36 cancers in 185 countries. *CA Cancer J Clin*. 2024;74(3):229–263. doi:10.3322/caac.21834
11. Xia C, Dong X, Li H, et al. Cancer statistics in China and United States, 2022: profiles, trends, and determinants. *Chin Med J*. 2022;135 (5):584–590. doi:10.1097/CM9.0000000000002108
12. Zhu J, Yuan Y, Wan X, et al. Immunotherapy (excluding checkpoint inhibitors) for stage I to III non-small cell lung cancer treated with surgery or radiotherapy with curative intent. *Cochrane Database Syst Rev*. 2021;12(12):CD011300. doi:10.1002/14651858.CD011300.pub3
13. Xu C, Chen YP, Du XJ, et al. Comparative safety of immune checkpoint inhibitors in cancer: systematic review and network meta-analysis. *BMJ*. 2018;363:k4226. doi:10.1136/bmj.k4226
14. Haratani K, Hayashi H, Chiba Y, et al. Association of Immune-Related Adverse Events With Nivolumab Efficacy in Non-Small-Cell Lung Cancer. *JAMA Oncol*. 2018;4(3):374–378. doi:10.1001/jamaoncol.2017.2925
15. Zhao LN, Yang YQ, Wang WW, Li Q, Xiao H. The effects of traditional Chinese medicine combined with chemotherapy on immune function and quality of life in patients with non-small cell lung cancer: a protocol for systematic review and meta-analysis. *Medicine*. 2020;99(45):e22859. doi:10.1097/MD.0000000000022859
16. Huang CY, Ju DT, Chang CF, Muralidhar Reddy P, Velmurugan BK. A review on the effects of current chemotherapy drugs and natural agents in treating non-small cell lung cancer. *Biomedicine*. 2017;7(4):23. doi:10.1051/bmdcn/2017070423
17. Chen YY, Chen CH, Lin WC, et al. The Role of Autophagy in Anti-Cancer and Health Promoting Effects of Cordycepin. *Molecules*. 2021;26 (16):4954. doi:10.3390/molecules26164954
18. Xu H, Li S. Pharmacological effects of Bailing capsule and its application in lung disease research. *Zhongguo Zhong Yao Za Zhi*. 2010;35 (20):2777–2781.
19. Cai H, Li J, Gu B, et al. Extracts of Cordyceps sinensis inhibit breast cancer cell metastasis via down-regulation of metastasis-related cytokines expression. *J Ethnopharmacol*. 2018;214:106–112. doi:10.1016/j.jep.2017.12.012
20. Zhu JS, Halpern GM, Jones K. The scientific rediscovery of an ancient Chinese herbal medicine: cordyceps sinensis: part I. *J Altern Complement Med*. 1998;4(3):289–303. doi:10.1089/acm.1998.4.3-289
21. Jin L, Jin L, Wu R, et al. Hirsutella Sinensis Fungus Regulates $CD8^+$ T Cell Exhaustion Through Involvement of T-Bet/Eomes in the Tumor Microenvironment. *Front Pharmacol*. 2021;11:612620. doi:10.3389/fphar.2020.612620
22. Su J, Sun J, Jian T, Zhang G, Ling J. Immunomodulatory and Antioxidant Effects of Polysaccharides from the Parasitic Fungus Cordyceps kyushuensis. *Biomed Res Int*. 2020;2020:8257847. doi:10.1155/2020/8257847
23. Saraiva M, Vieira P, O'Garra A. Biology and therapeutic potential of interleukin-10. *J Exp Med*. 2020;217(1):e20190418. doi:10.1084/jem.20190418
24. Saxton RA, Tsutsumi N, Su LL, et al. Structure-based decoupling of the pro- and anti-inflammatory functions of interleukin-10. *Science*. 2021;371 (6535):eabc8433. doi:10.1126/science.abc8433
25. Salkeni MA, Naing A. Interleukin-10 in cancer immunotherapy: from bench to bedside. *Trends Cancer*. 2023;9(9):716–725. doi:10.1016/j.trecan.2023.05.003
26. Shiri AM, Zhang T, Bedke T, et al. IL-10 dampens antitumor immunity and promotes liver metastasis via PD-L1 induction. *J Hepatol*. 2024;80 (4):634–644. doi:10.1016/j.jhep.2023.12.015
27. Jung YJ, Woo JS, Hwang SH, et al. Effect of IL-10-producing B cells in peripheral blood and tumor tissue on gastric cancer. *Cell Commun Signal*. 2023;21(1):320. doi:10.1186/s12964-023-01174-5
28. Wang X, Wang X, Wang D, et al. Interleukin-10 overexpression in 4T1 cells: a gateway to suppressing mammary carcinoma growth. *Int Immunopharmacol*. 2024;142(Pt A):113089. doi:10.1016/j.intimp.2024.113089
29. Sullivan KM, Jiang X, Guha P, et al. Blockade of interleukin 10 potentiates antitumour immune function in human colorectal cancer liver metastases. *Gut*. 2023;72(2):325–337. doi:10.1136/gutjnl-2021-325808
30. Zhang H, Li R, Cao Y, et al. Poor Clinical Outcomes and Immunoevasive Contexture in Intratumoral IL-10-Producing Macrophages Enriched Gastric Cancer Patients. *Ann Surg*. 2022;275(4):e626–e635. doi:10.1097/SLA.0000000000004037
31. Ma Y, Cui Q, Zhu W, et al. A Novel Tetramethylpyrazine Chalcone Hybrid- HCTMPPK, as a Potential Anti-Lung Cancer Agent by Downregulating MELK. *Drug Des Devel Ther*. 2024;18:1531–1546. doi:10.2147/DDDT.S449139
32. Li J, Zhang D, Wang S, et al. Baicalein induces apoptosis by inhibiting the glutamine-mTOR metabolic pathway in lung cancer. *J Adv Res*. 2025;68:341–357. doi:10.1016/j.jare.2024.02.023
33. Livak KJ, Schmittgen TD. Analysis of relative gene expression data using real-time quantitative PCR and the 2-Ct method. *Methods*. 2001;25 (4):402–408. doi:10.1006/meth.2001.1262
34. Fernandez-Santamaria R, Satitsuksanoa P. Engineered IL-10: a matter of affinity. *Allergy*. 2022;77(3):1067–1069. doi:10.1111/all.15132
35. Dallagi A, Girouard J, Hamelin-Morrissette J, et al. The activating effect of IFN-γ on monocytes/macrophages is regulated by the LIF-trophoblast-IL-10 axis via Stat1 inhibition and Stat3 activation. *Cell Mol Immunol*. 2015;12(3):326–341. doi:10.1038/cmi.2014.50
36. Bian G, Ding X, Leigh ND, et al. Granzyme B-mediated damage of CD8+ T cells impairs graft-versus-tumor effect. *J Immunol*. 2013;190 (3):1341–1350. doi:10.4049/jimmunol.1201554
37. Savid-Frontera C, Viano ME, Baez NS, et al. Exploring the immunomodulatory role of virtual memory $CD8^+$ T cells: role of IFN gamma in tumor growth control. *Front Immunol*. 2022;13:971001. doi:10.3389/fimmu.2022.971001
38. Liu Y, Weng W, Gao R, Liu Y. New Insights for Cellular and Molecular Mechanisms of Aging and Aging-Related Diseases: herbal Medicine as Potential Therapeutic Approach. *Oxid Med Cell Longev*. 2019;2019:4598167. doi:10.1155/2019/4598167
39. Xu F, Wei Y, Tang Z, Liu B, Dong J. Tumor-associated macrophages in lung cancer: friend or foe? *(Review) Mol Med Rep*. 2020;22(5):4107–4115.
40. Pan Y, Yu Y, Wang X, Zhang T. Tumor-Associated Macrophages in Tumor Immunity [published correction appears in Front Immunol. 2021 Dec 10;12:775758]. *Front Immunol*. 2020;11(11):583084. doi:10.3389/fimmu.2020.583084
41. Pearce OMT, Delaine-Smith RM, Maniati E, et al. Deconstruction of a Metastatic Tumor Microenvironment Reveals a Common Matrix Response in Human Cancers. *Cancer Discov*. 2018;8(3):304–319. doi:10.1158/2159-8290.CD-17-0284
42. Bockel S, Durand B, Deutsch E. Combining radiation therapy and cancer immune therapies: from preclinical findings to clinical applications. *Cancer Radiother*. 2018;22(6–7):567–580. doi:10.1016/j.canrad.2018.07.136

43. Qiu H, Hu X, Gao L, et al. Interleukin 10 enhanced CD8+ T cell activity and reduced CD8+ T cell apoptosis in patients with diffuse large B cell lymphoma. *Exp Cell Res*. 2017;360(2):146–152. doi:10.1016/j.yexcr.2017.08.036
44. Hanna BS, Llaó-Cid L, Iskar M, et al. Interleukin-10 receptor signaling promotes the maintenance of a PD-1int TCF-1^{+} CD8^{+} T cell population that sustains anti-tumor immunity. *Immunity*. 2021;54(12):2825–2841.e10. doi:10.1016/j.immuni.2021.11.004
45. Sun Q, Zhao X, Li R, et al. STAT3 regulates CD8+ T cell differentiation and functions in cancer and acute infection. *J Exp Med*. 2023;220(4): e20220686. doi:10.1084/jem.20220686
46. Naing A, Papadopoulos KP, Autio KA, et al. Safety, Antitumor Activity, and Immune Activation of Pegylated Recombinant Human Interleukin-10 (AM0010) in Patients With Advanced Solid Tumors. *J Clin Oncol*. 2016;34(29):3562–3569. doi:10.1200/JCO.2016.68.1106
47. Guedan S, Ruella M, June CH. Emerging Cellular Therapies for Cancer. *Annu Rev Immunol*. 2019;37(1):145–171. doi:10.1146/annurev-immunol-042718-041407
48. Goronzy JJ, Weyand CM. Mechanisms underlying T cell ageing. *Nat Rev Immunol*. 2019;19(9):573–583. doi:10.1038/s41577-019-0180-1
49. Farhood B, Najafi M, Mortezaee K. CD8+ cytotoxic T lymphocytes in cancer immunotherapy: a review. *J Cell Physiol*. 2019;234(6):8509–8521. doi:10.1002/jcp.27782
50. Hay ZLZ, Slansky JE. Granzymes: the Molecular Executors of Immune-Mediated Cytotoxicity. *Int J Mol Sci*. 2022;23(3):1833. doi:10.3390/ijms23031833
51. Zhao K, Ma Y, Luo J, et al. Hirsutella sinensis Fungus Promotes CD8+ T Cell-Mediated Anti-Tumor Immunity by Affecting Tumor-Associated Macrophages-Derived CCRL2. *Immunol Invest*. 2025;54(4):573–588. doi:10.1080/08820139.2025.2450246
52. Cerqueira C, Manfroi B, Fillatreau S. IL-10-producing regulatory B cells and plasmocytes: molecular mechanisms and disease relevance. *Semin Immunol*. 2019;44:101323. doi:10.1016/j.smim.2019.101323
53. Zhao Y, Wu T, Shao S, Shi B, Zhao Y. Phenotype, development, and biological function of myeloid-derived suppressor cells. *Oncoimmunology*. 2015;5(2):e1004983. doi:10.1080/2162402X.2015.1004983